Int. J. Electrochem. Sci., 16 **(2021)** Article Number: 211044, doi: 10.20964/2021.10.20

International Journal of
ELECTROCHEMICAL
SCIENCE
www.electrochemsci.org

Short Communication

Effect of *Azolla Imbricata* and *Spirodela Polyrrhiza* on Chromium(VI) Removal and Power Generation in a Plant Microbial Fuel Cell

Hong Ye[1], *Guangming Yang*[2,*]

[1] Planning and Finance Department, Chongqing Radio and TV University, Chongqing,400052, China;
[2] School of Management, Chongqing University of Technology, Chongqing, 400054, China
[*]E-mail: guangming_y688@126.com

Received: 31 May 2021/*Accepted:* 5 July 2021/*Published:* 10 September 2021

In this study, we performed a remediation of hexavalent chromium-contaminated soil within a constructed plant microbial fuel cell and vary the voltage to study its power generation stability. The maximum power density was driven to investigate the performance of systematic electricity generation. Furthermore, the concentration changes in total chromium and hexavalent chromium in the reactor effluent were used to study the effect of *Azolla imbricata* on the hexavalent chromium removal rate. The results showed that the plant group was 40–80 mV higher when compared with the non-plant group. The maximum power density of the *Azolla imbricata* group was 2.14 times higher than that of the non-plant group, indicating that the electricity generation performance of the plant group was markedly improved. Compared to the non-plant group, the total chromium and hexavalent chromium residue are only 10.1% and 8.1%, respectively, in the *Azolla imbricata* group. The synergistic effect of plants and the microbial cell noticeably quickens the hexavalent chromium removal. This work provided a novel strategy for the treatment of hexavalent chromium-contaminated soil.

Keyword: Hexavalent chromium; Plant microbial fuel cell; Electrochemistry; Synergistic effect

1. INTRODUCTION

With the rapid development of heavy industry, soil pollution has resulted in heavy metal chromium contamination becoming a serious environmental issue [1–3]. Hexavalent and trivalent chromium are the main forms of Cr occurring in natural environments. Hexavalent chromium is a particular concern given its significant role in widespread soil contamination and the fact that it cannot be degraded naturally [4]. Furthermore, hexavalent chromium shows high activity and cannot be easily adsorbed by soil, with free hexavalent chromium accumulations in biota resulting from transport and

diffusion in the soil, thereby presenting a threat to humans through the food chain [5]. Thus, tremendous efforts have been devoted to the search for low-cost and efficient hexavalent chromium degradation technologies.

Hexavalent chromium is usually converted to trivalent chromium, which can effectively reduce its toxicity and diffusion to complete the restoration of Cr-contaminated soil [6,7]. Gao et al. used a ferric chloride citric acid complex solution to leach heavy metal-contaminated soil and it effectively removed the toxic heavy metal Cr in the soil [8]. With the development of bioremediation technology, Cui et al. found that the degradation efficiency for *Cyperus alternifolius* to hexavalent chromium was as high as 97.0% with a strong enrichment of Cr(VI) [9]. However, these methods cannot be applied to the large-scale remediation of contaminated soil [10,11]. For example, the chemical leaching technology is not only energetically costly but also has the potential contribute to secondary pollution [12]. Simultaneously, bioremediation technology also presents a slow remediation rate and the different plants present differences in the remediation effects for contaminated soil [13]. The above-mentioned studies showed that the development of traditional remediation techniques entered a bottleneck, while the bioremediation technology also had enormous development potentials, which needed to be further investigated and developed.

As microbial fuel cell (MFC) research development advances, MFCs can be used to derive energy from heavy metal-polluted soil or wastewater, with clear green and sustainable motivations [14]. Liu et al. constructed a double-chamber MFC that was used to generate electricity while removing Cu^{2+} ions from copper wastewater with a removal rate of up to 80% [15]. Zhuang et al. utilized a MFC in the treatment of zinc wastewater and in the case of external a resistance of 10 Ω, the Zn^{2+} ion removal rate in the cathodic compartments was 35% after 192 h [16]. Furthermore, the experiments demonstrated that the MFC was capable of governing heavy metal pollution effectively while providing access to green energy. Nevertheless, the use of pure MFCs is still restricted and cannot be easily scaled up. Although MFCs are green and eco-friendly, they require long reaction periods for heavy metal pollution. Furthermore, current research is limited for the application of MFCs to the remediation of toxic heavy metals from the soil, such as the restoration of Cr(VI)-contaminated soil [17].

Based on the above research, it was hypothesized that MFCs combined with plants could be a possible pathway for increasing the remediation efficiency of contaminated soil and obtaining stable energy generation. The present study investigated a novel system for combined remediation using microbes and plants for Cr(VI)-contaminated soil with a green and environmentally-friendly energy source. We used a newly constructed plant microbial fuel cell (PMFC) to explore *Azolla imbricata*, *Spirodela polyrrhiza* and a non-plant group for different hydraulic retention times (HRTs). We test the effluent quality parameters, including total nitrogen (TP), total phosphorus (TN), total Cr and Cr(VI), to investigate the repair situation of contaminated soil. In addition, the influence of the testing voltage, power density and polarization of the system on the electricity generation performance was considered. Our constructed PMFC provided a novel solution for the restoration of Cr(VI)-contaminated soil.

2. EXPERIMENTAL

2.1 Construction of experimental device

The experimental system used in this study is presented in Figure 1 and comprised a reaction vessel, leachate collector and liquid circulation system. The size of the reaction vessel was 150 × 100 × 150 mm. The reactor layered structure was ordered from top to bottom with soil, carbon cloth, soil, activated carbon rolling steel mesh and water layers. The carbon cloth layer was soaked in acetone for more than 12 h and then dried in a muffle oven for 2 h. The activated carbon rolling steel mesh layer was used as a cathode and the carbon cloth layer as an anode. An additional resistance of 1,000 Ω was added between the cathode and anode. The plant was planted in a circular hole in the middle of the cathode. In order to ensure that the plant rhizosphere secretion was used by the microorganisms on the anode to the greatest extent, the root must be as close to the anode as possible. In addition, the size of the leachate collector was 10 cm in diameter and 2 cm in height. The soil leachate collected during the leachate collector was transported back to the top of the reactor by a BT100-2J peristaltic pump (Lange Peristaltic Pump Inc., Baoding, China).

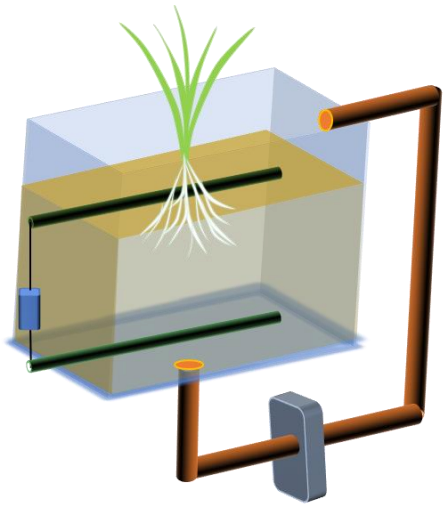

Figure 1. Schematic of a plant microbial fuel cell.

2.2 Preparation of experimental sample

Soil samples were collected from six areas in the Simian Mountain of Chongqing and dried naturally in a ventilated location indoors. After mixing, the animal and plant residues and stones were removed and the soil was ground with a wooden hammer until it passed through a 100-mesh sieve and stored in a sealed plastic bag for analysis and determination. In order to enable the reactor to accumulate more microorganisms as soon as possible in a relatively short period of time and reach a stable state of electricity production as soon as possible, this experiment utilized 300 mL of sludge from a primary sedimentation tank (Chengbei Sewage Co. Ltd., Chongqing, China).

Before planting the plants, 500 mg of potassium perchromate were added per kg of soil specimen (soil chromium content of 500 mg/kg) and mixed, which facilitated an even distribution of Cr(VI) throughout the soil specimen. High concentrations of Cr also amplified the experimental effects.

One compartmental MFC was employed as a reactor in this assay and the HRT was used as the variable and was controlled via a peristaltic pump. The water used in the experiment was distilled water, which prevented other factors interfering with the experimental results and supplements the natural water evaporation. A nutrient solution was also added, which was used at normal plant and microorganism growths, including 50 mL of a 50 mM phosphoric acid buffer salt solution, as shown in Table 1, 12.5 mL of a mineral element solution (as shown in Table 2) and 0.5 mL of a vitamin mother liquor.

Table 1. Composition of 50 mM phosphate buffer solution

Component	Concentration (g/L)
NH_4Cl	0.35
KCl	0.12
$NaH_2PO_4 \cdot 2H_2O$	2.67
$Na_2HPO_4 \cdot 12H_2O$	11.3

Table 2. Composition of mineral element solution

Component	Concentration (g/L)
$MgSO_4 \cdot 7H_2O$	3.00
$CoCl_4 \cdot 6H_2O$	0.21
NTA	1.56
$ZnSO_4 \cdot 7H_2O$	0.25
NaCl	1.05
$CaCl_2 \cdot 2H_2O$	0.25
$MnSO_4 \cdot H_2O$	0.51
$CuSO_4 \cdot 5H_2O$	0.02

Azolla imbricata and *Spirodela polyrrhiza* were selected as the experimental plants and acclimated in the deionized water for 10 d. We opted for healthy plants with consistent growth and similar morphologies to implant into different reactors. Three groups were divided into the reactor of *Azolla imbricata*, *Spirodela polyrrhiza* and the non-plant group in the first phase and testing its treatment effect when HRT was 5, 10 and 15 h, respectively. After the first stage, we found that *Spirodela polyrrhiza* relative to *Azolla imbricata* had better ability for electricity generation and the removal of hexavalent chromium. We divided the reactor of *Spirodela polyrrhiza* and the non-plant group into two groups in the second stage and tested the treatment effects of different HRTs in the same manner.

2.3 Measurement and calculation

The voltage was obtained using the applied voltage of additional resistance. Data acquisition was used to record the voltage of the applied resistance every 10 min. The current density I (mA/m^2) is given by:

$$I = U/(R \cdot A) \quad (1)$$

where U is the system output voltage (V), R is the applied resistance and A is the area of the anode.

The power density (P) of the MCFC can be determined by the maximum power density curve as:

$$P = U \cdot U/(R \cdot A) \quad (2)$$

Meanwhile, the pH, dissolved oxygen and total nitrogen (TN) in the effluent were measured using a pH meter (PHBJ-260F, Leici Co. Ltd., Shanghai), portable handheld dissolved oxygen meter (JPBJ-608, Leici Co. Ltd., Shanghai) and TN analyzer (GL-200, GLKRUI Co. Ltd., Shandong), respectively. Meanwhile, the hexavalent chromium in the effluent was measured using a diphenyl carbazide ($C_{13}H_{14}N_4O$) spectrophotometric determination at 540 nm. The concentrations for the total Cr and total phosphorus (TP) were determined using inductively coupled plasma-optical emission spectrometry, while the trivalent Cr concentrations were obtained by subtracting the Cr(VI) concentrations from the total Cr concentrations.

3. RESULTSs AND DISCUSSION

The process of the reactor startup is dependent on the change in voltage and the voltage during the priming phase at a hydraulic retention time of 10 h, as shown in Figure 2. The result showed that the three-group reactors could all be primed successfully and generate stable power. Compared with the non-plant group, the plant group reached the system stabilization period faster, meaning that plant presence was effective at promoting the starting speed of the soil MFC. It is noteworthy that the *Azolla imbricata* group reached the highest voltage at 409 h, which was faster than the other groups and could have resulted from the large surface area of its root and its large contact area with the anode [18].

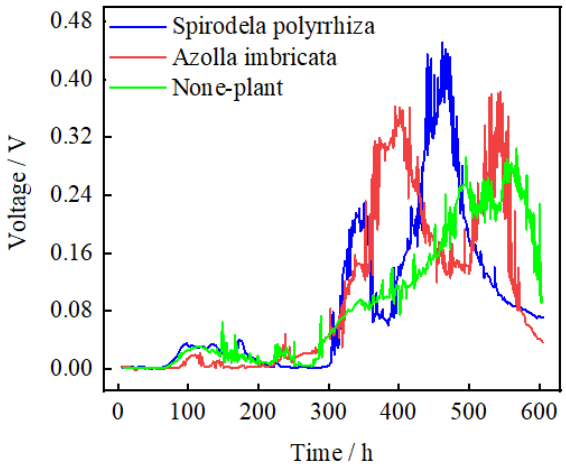

Figure 2. Voltage diagram during operation. The voltage of the external resistance is recorded every 5 min and measured by a multi-channel data acquisition instrument (model 2700, Keithley Inc, USA).

The system voltage curves are shown in Figure 3. The HRT was selected as 15, 10 and 5 h in this experiment and each change in HRT required 30 min to stabilize. With the PMFC in this study occurring in soil, its voltage plot was different from the voltage plot of the MFC in water [19]. The time-voltage curves appeared ordered and regular, with waveform changes exhibited. When the hydraulic retention time was 15 h, the maximum output voltages of the *Azolla imbricata*, *Spirodela polyrrhiza* and non-plant groups were 360, 420 and 320 mV, respectively. When the HRT was ~10 h, the maximum output voltage was significantly increased in all groups (the maximum output voltages of the *Azolla imbricata*, *Spirodela polyrrhiza* and non-plant groups were 360, 420 and 320 mV, respectively).

Importantly, by comparing the output voltage of the specimens, the *Azolla imbricata* reactor was found to have the maximum output voltage, which was 1.21 times higher than the output voltage of the non-plant group. This result strongly implied that presence of plants clearly enhanced the output voltage of the reactor. In addition, the output voltage of the *Spirodela polyrrhiza* group gradually decayed with HRT, indicating that *Spirodela polyrrhiza* was not suitable for long-term growth under this condition. Despite this, *Spirodela polyrrhiza* still maintained the power generation capacity.

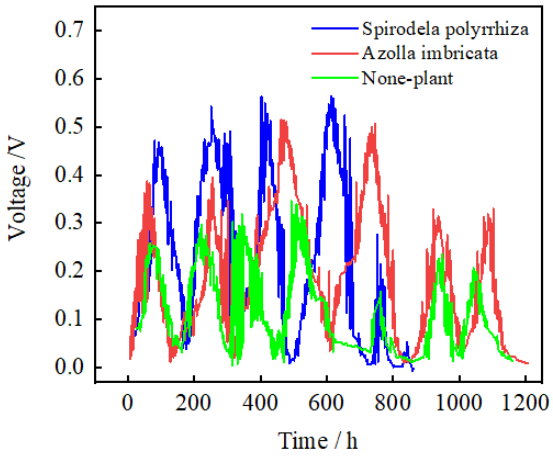

Figure 3. Voltage diagram of operation phase. Hydraulic retention time was selected as 15, 10 and 5 h in this experiment.

The power density of the reactor is shown in Figure 4(a). It was found that the power density decreased after an initial increase with increasing current density. The different HRTs had a significant influence on the maximum output power of the reactor. When the HRT was 5, 10 and 15 h, the maximum output powers of the *Azolla imbricata* group were 18.11, 29.68 and 20.57 W/m^2, respectively. Importantly, the difference in maximum power density indicated the difference in actual power generation ability and the maximum power density of *Azolla imbricata* even reached 2.14 times that of the non-plant group, indicating that the presence of plants clearly enhanced the power generation ability of the reactor.

The polarization curves of the reactor are shown in Figure 4(b). The voltage declined as the current density increased and the discharge processes of the three reactors are relatively smooth. This indicated that the anodes formed stable biofilms, with the three reactors displaying comparative stability.

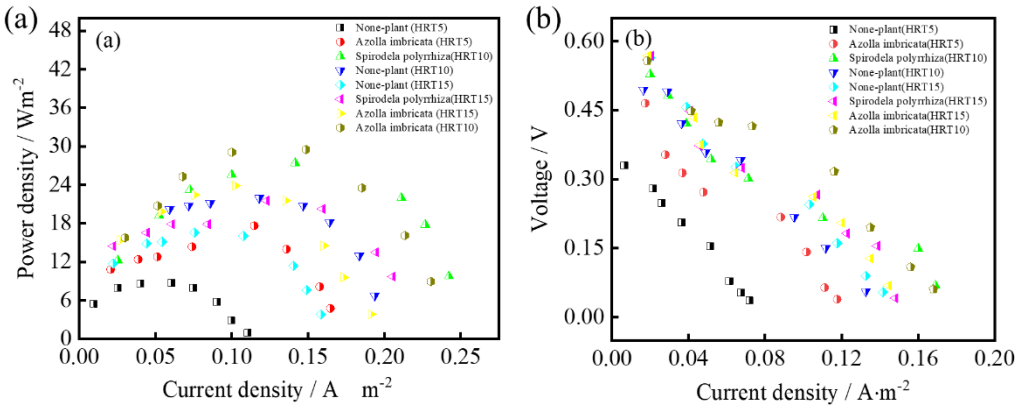

Figure 4. Effect of different plants on reactor (a) power density and (b) polarization curves under different HRTs.

One of most important factors for the activity of electrogenic bacteria is pH. Some studies have illustrated that most crops thrive in soils that are neutral (pH 7) or slightly acidic [20]. The pH of the system is altered during the reaction and it is noteworthy that the valence state of chromium in soil is closely related to pH. According to a previous report [21], pH is also one of the determinants of Cr adsorption in soil and Cr(VI) degradation.

The change in reactor pH was determined serially from the starting phase, as illustrated in Figure 5(a). The pH of the none-plant group was slightly higher than the pH of the *Azolla imbricata* group and it reached the highest level at a HRT of 10 h. Moreover, the reaction took place under weak alkaline conditions, in contrast to previous investigations that suggested that acidic environments were more suitable for hexavalent chromium reduction. The outstanding chromium reduction performance was attributed to the biocatalysis of cathode microorganisms. Based on the above results, this reactor did not need pH adjustment, which will help to reduce the cost of hexavalent chromium removal.

The results for dissolved oxygen (DO) reflected the operation state of the reaction system. DO is made primarily for microbial metabolism and is redox reactive. In this experiment, the reactor was run in circulation flows and the DO in the incoming water was 3.7 mg/L on average. As shown in Figure 5(b), the DO content became larger as the HRT was shortened. Simultaneously, the DO of the *Azolla imbricata* group was significantly higher than the DO of the none-plant group, suggesting that the plant improved the oxygen supply within the soil.

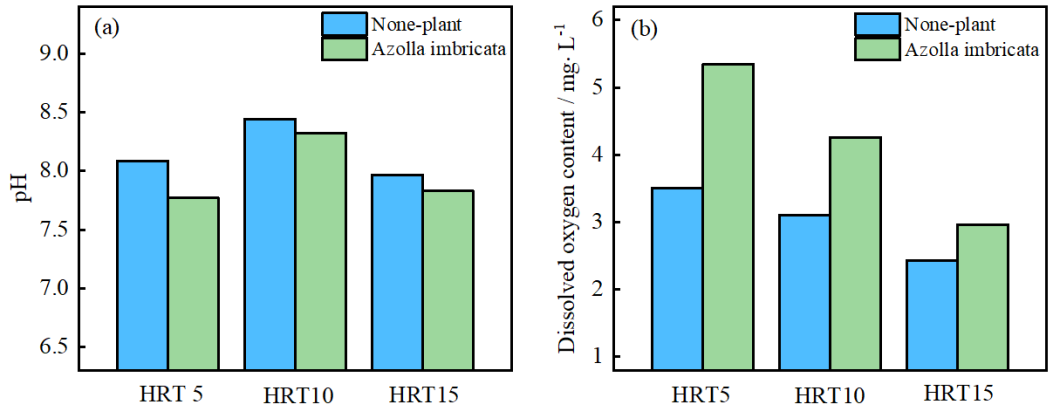

Figure 5. Influence of plant on the change of (a) pH and (b) dissolved oxygen in the reaction process.

It has been well documented that the nitrogen content determined the plant growth efficiency. The TN in the reactor yielding water was determined serially and is displayed in Figure 6(a). The TN content in the reactor with incoming water was 83.852 mg/L on average and it continued to decrease, with a final TN concentration for the none-plant group in yielding water of 9.94 mg/L and a removal rate of TN of 87.52%. The final TN concentration of the *Azolla imbricata* group in yielding water was 6.22 mg/L, with a removal rate of 92.33%. The results demonstrated that the TN of the plant group was always less than the TN of the none-plant group. Due to the absorption of nitrogen from the plant, some nitrogen metastasized to plant. In addition, the plant was stimulated in response to the MFC, which strengthened the nitrogen utilization.

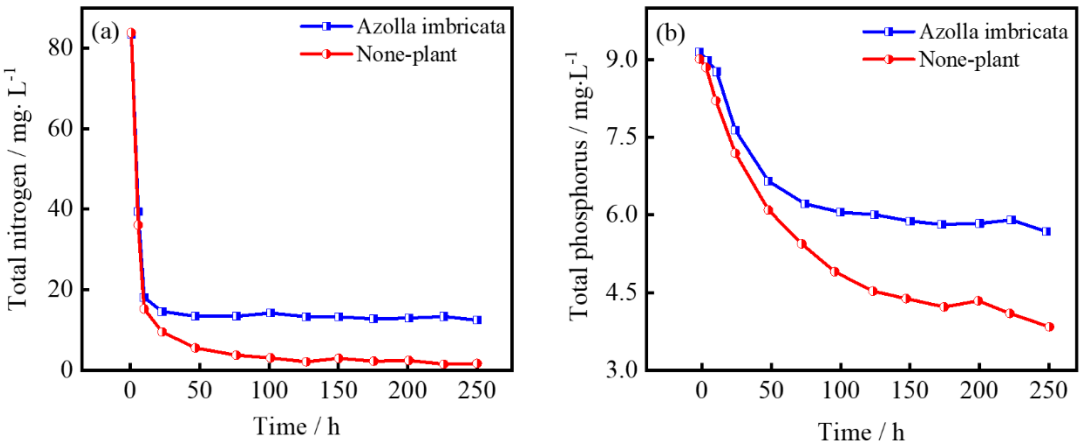

Figure 6. Influence of plant on the change of (a) total nitrogen and (b) phosphorus in the reaction process.

Furthermore, phosphorus-accumulating bacteria in soil accumulated phosphorus in aerobic environments. As presented in Figure 6(b), the TP concentration in incoming water was 9.12 mg/L. The TP concentration significantly decreased with or without the plant during the initial stage, which was mainly due to the intercept of the soil and electrode. As the experiment progressed, the TP concentration in the plant group was always lower than the TP concentration in the none-plant group. This resulted not only from the uptake of phosphorus by the plant, but also from the plant root secreting oxygen, which

led to the formation of anaerobic, aerobic and hypoxia status, favoring the bacterial treatment of phosphorus.

The changes in the total and hexavalent chromium concentrations are presented in Figure 7(a). In this experiment, hexavalent chromium was mainly removed by cathodic electrochemical reduction, phytoconcentration and directly to microbe reduction and electrode adsorption.

After running the reactor, it can be seen that total and hexavalent chromium concentrations decreased rapidly due to the intercept and adsorption of the anode and cathode materials. Even more impressively, the total and hexavalent chromium concentrations of the *Azolla imbricata* group were significantly lower than those of the none-plant group. This was because the root exudates provided more electronics for the reduction of hexavalent chromium and served to promote the bioelectrochemical conversion of hexavalent chromium to trivalent chromium. Hexavalent chromium received electrons from the oxidation of anode organic matter and was reduced to trivalent chromium on the cathode via [22]:

$$Cr_2O_7^{2-}+14H^++6e^-\rightarrow 2Cr^{3-}+7H_2O \quad (3)$$

It can be seen from Figure 7(b) that the adsorption of the electrode in the none-plant group proportionate reductions in the concentration of chromium concentration and hexavalent chromium was transformed into nontoxic trivalent chromium in the electrochemical system.

In addition, the chromium removal efficiency and maximum output power compared with similar results are shown in Table 3. *Azolla imbricata* had a higher removal rate of Cr(VI) and a high maximum output power, which implied that it had excellent potential for the degradation of Cr(VI).

Table 3. Chromium removal efficiency and maximum output power compared with similar results

Samples	Chromium removal efficiency	Maximum output power
MFC, Anaerobic sludge [23]	85.2 %, 150 h	0.15 W/m^2
MFC, electroplating wastewater [24]	90.3 %, 25 h	1.6 W/m^2
Spartina-PMFC [25]	87.2 %, 142 h	222 mW/m^2
Rice-PMFC [26]	82.0 %, 50 h	6 mW/m^2
Reed-PMFC [27]	85.6 %, 60 h	110 mW/m^2
Our works	91.9 %, 125 h	29.68 W/m^2

Simultaneously, the use of *Azolla imbricata* in the MFC accelerated the reduction of hexavalent chromium. With part of the chromium fixed with the plant root and enriched to the plant, the chromium content in yielding water was dramatically reduced. The total and hexavalent chromium final concentrations of the *Azolla imbricata* group (0.301 and 0.177 mg/L, respectively) were less than those of the none-plant group (2.968 and 2.169 mg/L, respectively). Hence, the presence of *Azolla imbricata* accelerated the total and hexavalent chromium removal.

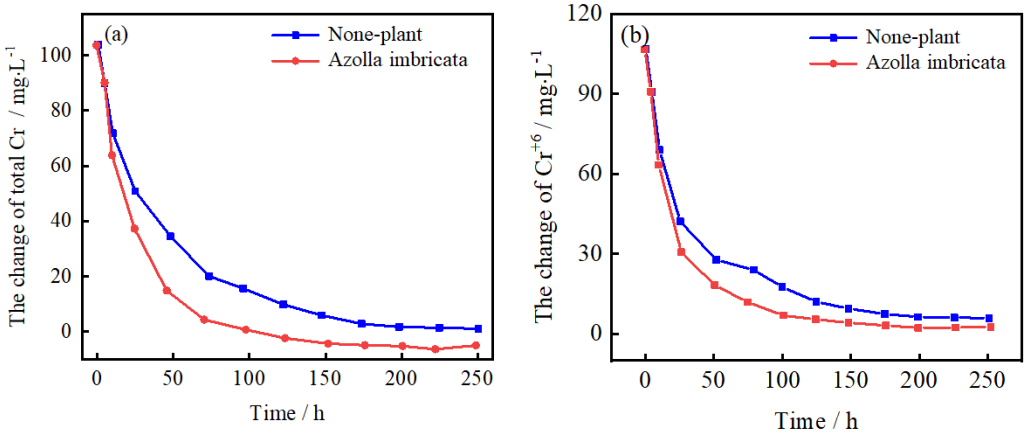

Figure 7. Changes in (a) total and (b) hexavalent chromium concentrations after adding *Azolla imbricata*.

4. CONCLUSION

This study focused on the startup of a microbial fuel cell with *Azolla imbricata* and *Spirodela polyrrhiza* and the effect of these two plants on the reactor in three HRTs. These plants could accelerate the initiation speed of the reactor and improve the effects of power generation. At a HRT of 10 h, the power generation of the *Azolla imbricata* group reached 2.14 times that of the none-plant group and the power generation efficiency reached a maximum. In parallel, too slow or too fast HRTs were detrimental to the electricity generation of the reactor. From the pH of the reactor, this experiment was operated in neutral or alkaline environments, where traditional method cannot operate and it can effectively decrease the costs. The oxygen secretion in the plant root formed aerobic and hypoxic zones, which facilitated the uptake of nitrogen, phosphorus by the reactor and the contents of nitrogen and phosphorus in the plant group effluent were much lower than those in the none-plant group. Furthermore, the contents of hexavalent chromium and total chromium in plant group effluent were also much lower than those in the none-plant group, the existence of plant promoted the chromium removal efficiency in reactor. This study provided a novel solution for the restoration of Cr(VI)-contaminated soil.

ACKNOWLEDGEMENTS
This work was supported financially by the Commission Science and Technology Project of Chongqing Education (Grant No. KJQN201904002).

References

1. Y. G. Liu, W. H. Xu, G. M. Zeng, X. Liu and H. Gao, *Process Biochem.*, 9 (2006) 1981-1986.
2. B. Jiang, Y. F. Gong, J. N. Gao, T. Sun, Y. J. Liu, N. Oturan and M. A. Oturan, *J. Hazard. Mater.*, 365 (2019) 205-226.
3. S. P. Xia, Z. L. Song, P. Jeyakumar, S. MD. Shaheen, J. Rinklebe, Y. S. Ok, N. Bolan and H. L. Wang, *Crit. Rev. Env. Sci. Tec.*, 49 (2019) 1027-1078.
4. B. A. Marinho, R. O. Cristóvão, R. Djellabi, J. M. Loureiro, R. A. R. Boaventura and V. J. P. Vilara,

Appl. Catal. B-Environ., 203 (2017) 18-30.
5. A. S. Ellis, T. M. Johnson and T. D. Bullen, *Science*, 295 (2002) 2060-2062.
6. S. Deng and R. Bai, *Water Res.*, 38 (2004) 2424-2432.
7. V. S. Protsenko and F. I. Danilov, *Clean Technol. Envir.*, 16 (2014) 1201-1206.
8. J. B. Gao, J. Zhao, C. X. Dong, L. H. Wu and P. J. Hu, *J. Soil. Sediment.*, 18 (2018) 1020-1028.
9. L. H. Cui, Y. Ouyang, Y. Chen, X. Z. Zhu and W. L. Zhu, *Ecol. Eng.*, 35 (2009) 1271-1274.
10. M. P. Castro, F. R. D. Moraes, R. Y. Fujimoto, C. D. Cruz, M. A. D. A. Belo and J. R. E. D. Moraes, *B. Environ. Contam. Tox.*, 92 (2014) 213-219.
11. R. Saha, R. Nandi and B. Saha, *J. Coord. Chem.*, 64 (2011) 1782-1806.
12. D. H. Wang, G. H. Li, S. Q. Qin, W. G. Tao S. H. Gong and J. Wang, *Ecotox. Environ. Safe.*, 208 (2021) 111734.
13. S. Mishra, R. N. Bharagava, *J. Environ. Sci. Heal. C*, 34 (2016) 1-32.
14. L. P. Huang, J. W. Chen, X. Quan and F. L. Yang, *Bioproc. Biosyst. Eng.*, 33 (2010) 937-945.
15. W. P. Liu and X. F. Yin, *Int. J. Min. Met. Mater.*, 24 (2017) 621-626.
16. L. Zhuang, Y. Zheng, S. G. Zhou, Y. Yuan, H. R. Yuan and Y. Chen, *Bioresource Technol.*, 106 (2012) 82-88.
17. B. H. Kim, I. S. Chang and G. M. Gadd, *Appl. Microbiol. Biot.*, 76 (2007) 485-494.
18. 18. B. Liu, M. Ji and H. Zhai, *Chemosphere*, 209 (2018) 739-747.
19. C. Y. Guan, Y. H. Tseng, D. C. W. Tsang, A. Y. Hu and C. P. Yu, *J. hazard. Mater.*, 365 (2019) 137-145.
20. G. C. Gil. I. Chang, B. H. Kim, M.Kim, J. Jang, H. S. Park and H. J. Kim, *Biosens. Bioelectron.*, 18(2003): 327-334.
21. D. P. Strik, H. V. M. Hamelers, J. F. H. Snel, and C. J. N. Buisman, *Int. J. Energ. Res.*, 32 (2008) 870-876.
22. X. He, B. Hou, C. Li, Q. Y. Zhu, Y. M. Jiang and L Y. Wu, *Electrochim. Acta*, 130 (2014) 245-252.
23. G. Wang, L. Huang and Y. Zhang, *Biotechnol. Lett.*, 30 (2008) 1959-1966.
24. Z. Li, X. Zhang and L. Lei, *Process Biochem.*, 43(2008) 1352-1358.
25. R. A. Timmers, D. P. Strik, H. V. M. Hamelers and J. N. B. Cees, *Appl. Microbiol. Biot.*, 86 (2010) 973-981.
26. N. Kaku, N. Yonezawa, Y. Kodama and K. Watanabe, *Appl. Microbiol. Biot.*, 79(2008) 43-49.
27. D. P. Strik, H. Terlouw, H. V. M. Hamelers and J. N. B. Cees, *Appl. Microbiol. Biot.*, 81(2008) 659-668.